Effects of Cu addition on creep characteristics of Sn–9Zn lead-free solders

M. Y. Salem
Physics Department, Faculty of Science at New Valley, Assuit University, 72511, El-Kharga, Egypt
Email: mahmoud_salem569@yahoo.com

Abstract: *In the present study, the transient, and steady state creep of Sn–9Sn and Sn–9Sn-0.7Cu ternary alloy was investigated in the temperature range from 323, to 403 K at different five stresses ranged from 3.62 to 11.22 MPa. The transient creep parameters n and β were found to be markedly affected by the creep test conditions, T and σ. The parameter β was found to be increased by increasing transformation temperature, also; n was found to increase by increasing T irrespective of the applied stress. The steady-state creep rate ε'_{st} was found to increase with increasing both T and σ for two alloys. The relationship between steady-state creep rate ε'_{st} and the stress is $\varepsilon'_{st} = C\sigma^m$ where $m=(\partial ln\varepsilon'_{st}/\partial ln\sigma)$, is the strain rate sensitivity parameter. This exponent is increased with increasing T in both alloys. Addition of small amount of 0.7Cu to the binary alloy increased its creep resistance and ductility and was found to be enhancing the plasticity of the ternary alloys. This behavior was attributed to the formation of the intermetallic compounds (IMCs) Sn_5Zn_8 and Cu_6Sn_5 during solidification. These IMCs played the role of pinning action for the moving dislocations and consequently leading to the increase of its creep resistance. Micro-structural changes were investigated by Optical microscope (OM), and X-ray diffraction.*

Keywords: *Binary alloy; Steady state creep; Ternary alloy; Transient creep.*

I. Introduction

Eutectic Sn–9Sn alloy is the alloy of choice for the solder spheres used in Ball Grid Array (BGA) and fine ball grid array (FBGA) of the most popular packaging technologies. They used in microelectronics industry because of the even shrinking device size and increasing number of circuits and thus, increasing need for input/output interconnects for processors [1-3]. These packages are the technology for both single and multi-chip module products. Recently, there has been a considerable interest in the reliability and lifetime of solder joints which are used extensively in surface mount technology (SMT) [4].

Sn–9Zn alloy is much attention and emerged as possible replacements for Sn-Pb solders because of its low melting point, excellent mechanical properties and low cost. However, its main disadvantage of poor oxidation resistance and wetting properties caused by the high activity and corrosion susceptibility of Zn prevents its wide practical usage, especially in the critical part of electronic packaging products. Studies on the properties of their overall wetting and mechanical properties have been widely investigated and progress has been made by adding different alloying elements, such as Ag, Cu [5–10].

It is well known that Sn-Zn solder alloys exhibit strong time-dependent deformation behavior, and the mechanical response of the solder can be controlled by varying their structural state, in particular, the grain boundary area and the addition of various alloying elements [11,12]. Since the creep is one of the most common and important micromechanical deformation mechanisms in solder joints, it is necessary to find out how the creep parameters changing with alloying additions, structural transformations and applied stresses. Previous studies showed that the proper addition of Cu in Sn–Zn solders is effective way to avoid the formation of IMCs between the interface with Sn-Zn [5,6].

The present paper, therefore, aims to describe the creep behavior the eutectic Sn-9Zn alloy in which 0.7Cu was added to form the respective ternary Sn-9Sn-0.7Cu solder alloy. The tensile creep behavior of the two alloys has been studied, at different strain rates and temperatures to compare the results with the eutectic Sn-9Zn. The selection of this alloy system was motivated in part by the attractive potential of the IMCs phases in structural applications. The reason why Cu enhances (or not) the plasticity in the ternary alloys has been analyzed.
X-ray analysis, optical microscopy (OM), and Cu-addition on the creep behavior had been discussed.

II. Experimental Procedures

In the present work, the lead-free solder alloys with the compositions of eutectic Sn–9Zn, Sn-9Zn-0.7Cu were prepared from Sn, Zn, and Cu (purity 99.99) as raw materials. The process of melting was carried out in a vacuum arc furnace under a high purity argon atmosphere to produce rod-like specimen of 50 mm in gauge length and 0.8 mm in cross-section diameter. The specimens were annealed at 453 K for 2 h and then slowly cooled to room temperature at a cooling rate equal $2x10^{-2}$ Ks^{-1}. After this heat treatment, the samples were annealed at room temperature for 1 week before testing. This procedure permitted a small amount of grain growth and grain stabilization to occur [13]. A cooling rate was achieved, so as to create the fine microstructure typically found in small solder joints in microelectronic packages [8].
Tensile creep tests were then performed under constant stresses ranging from 3.62 to 11.22 MPa, and at temperatures ranging from 323 to 403 K in 20 K increments for both alloys, with an experimental error of less than ± 3% [11]. The sensitivity of strain measurements was approximately $\pm 1.0 \times 10^{-2}$ and the accuracy of temperature measurements is of the order of ±1 K. The environment chamber temperature could be monitored by using a thermocouple contacting with specimen.
The creep tests have been extended to cover the three stages of creep regime. The evolution of microstructure for all solder alloys and phase identification of the alloy samples were carried out by X-ray diffractometry (XRD) at 40kV and 20 mA using Cu Kα radiation with diffraction angle (2θ) from 20.01^0 to 99.99^0 and a constant scanning speed of 1^0 /min.

III. Results and Discussion

3.1. Features of creep curves
3.1.1. Transient stage

According to the Sn-Zn binary phase diagram see Fig.(1), the equilibrium microstructure of the eutectic Sn-9Zn consists of the eutectic mixture of Sn-rich (close to pure Sn) phase and the Zn-rich phase. Addition of 0.7Cu to binary alloys form the respective ternary Sn-9Sn-0.7Cu solder alloy which are much higher (more superplastic) than those of the binary [14].

Fig.(2) shows the XRD results of the as-cast Sn–9Zn and Sn–9Zn–0.7Cu experimental alloys. In general, all the as-cast experimental alloys are mainly composed of β-Sn phase and precipitated Sn_5Zn_8 phase. However, the alloys containing Cu exhibited additional IMCs such as Cu_6Sn_5.

The OM images of the two alloys are presented in Fig.(3). In Fig.(3a), a typical eutectic Sn-9Zn microstructure composed of light gray areas of Sn_5Zn_8 IMCs and dark network-like eutectic regions of β-Sn grain boundaries. In Fig.(3b), the appropriate content of Cu in the Sn–9Zn solder was found to improve the microstructure of the alloy. The primary Cu_6Sn_5 IMCs might act as heterogeneous nucleation sites for β-Sn dendrites upon solidification and are able to refine the grain size of Sn–9Zn alloy. Consequently, the mechanical properties of Sn–9Zn–0.7Cu solder may be enhanced as can be seen later.

Concerning the creep curve, the transient strain is mostly described by the well-known equation [15]:

$$\varepsilon_{tr} = \beta t^{n} \qquad (1)$$

where ε_{tr} and t are the transient creep strain, and time, β and n are constants depending on the experimental test conditions.

The specific features of the creep for lead-free solder alloys Sn–9Zn eutectic and Sn–9Zn-0.7Cu alloys are compared as shown in Fig.4 (a)-(e). The trend in the creep curves at all the five levels of applied stresses suggests a rapid transition from a short primary creep regime, to a steady state and tertiary creep regime. The relation between $\ln\varepsilon_{tr}$ and lnt gives straight lines as shown in Fig.5(a)-(e). Slopes of these straight lines gave the values of the transient creep time exponent n and was found to have values ranging from 0.428 to 1.094 for Sn-9Zn binary alloy, and from 0.48 to 1.11 for Sn-9Zn-0.7Cu ternary alloys. It was found that n increases with increasing deformation temperature for both alloys as shown in Fig.(6), while their intercepts at lnt = 0 gave the transient creep parameter β, it was calculated from Eq. (2):

$$\ln\beta = (\ln t_2\, \varepsilon_{tr1} - \ln t_1 \varepsilon_{tr2})/\ln t_2 - \ln t_1 \qquad (2)$$

The parameter β was found to increase with increasing temperature and applied stress as shown in Fig.(7), it was found to exhibit values ranging from -11.46 to -4.93 for Sn-9Zn binary alloy, and from -11.66 to -6.6 for Sn-9Zn-0.7Cu ternary alloys as shown in Table (4-1).

Fig.(8) illustrates the relation between $\ln\varepsilon_{tr}$ and 1000/T at low temperature for Sn-9Zn eutectic and Sn-9Zn-0.7Cu alloys for five different applied stresses. These results yield activation enthalpies of 20.16 and 28.82 KJ/mole for Sn-9Zn eutectic in low and high temperature regions. The activation enthalpies for Sn-9Zn-0.7Cu alloys were 18.14 and 26.02 KJ/mole in low and high temperature regions as shown in Fig.(8,9). It is clear that activation enthalpies for Sn-9Zn binary alloys are more than ternary Sn-9Zn-0.7Cu alloys in low and high temperature regions because of ternary alloys are more refine in grain size and superplastic than binary alloys.

Table (4-1): Comparison of the transient creep characteristics of the tested alloys.

Materials	Exponent n	β	Q ($kJmol^{-1}$)
Sn-9Zn	0.428 : 1.094	-11.46 : -4.93	20.16 : 28.82
Sn-9Zn-0.7Cu	0.48 : 1.11	-11.66 : - 6.6	18.14 : 26.02

3.1.2. Steady-state creep stage

The steady-state strain rate $\acute{\varepsilon}_{st}$ of the tested samples is calculated from the slopes of the linear parts of the obtained creep curves Fig.(4). It increases with increasing the temperature and stress in two alloys as shown in Fig.(10, a and b). It can be seen that under the same test conditions the ternary alloy showed higher strain rate $\acute{\varepsilon}_{st}$ compared with that of the binary one. It can be seen that each curve is characterized by all the three characteristic regions: (I) primary, (II) secondary or steady state, and (III) tertiary. Since the stress and temperature are constants, the variation in creep rates, $\dot{\varepsilon}$, suggests a basic change in the internal structure of the alloy during time. The strain ε and strain rate $\dot{\varepsilon}$ are, in general, lower for Sn-9Zn eutectic samples than for Sn–9Zn-0.7Cu samples in spite of the applied stress, because of refine the grain size of the ternary. Such differences in the creep behavior may be related to the difference in the grain size between the two alloys. This result, together with the fact that no temperature dependence of strain at the minimum creep rate, suggests that the creep behavior is strongly affected by the Cu-addition. Furthermore, the obtained minimum creep rates are not affected by the creep weakening factor of dynamic recrystallization [16].

The variation of the transient creep parameter lnσ, (where σ is the stress) with the steady state creep $\ln\dot{\varepsilon}_{st}$ for different applied stresses for Sn-9Zn eutectic and Sn-9Zn-0.7Cu alloys is shown in Fig.(11). The value of strain rate sensitivity parameter m calculated from the

slopes of these straight lines, and was found to have values ranging from 0.24 to 0.356 for Sn-9Zn binary alloy, and from 0.26 to 0.373 for Sn-9Zn-0.7Cu ternary alloys as shown in Fig.(12). It is shown that the value of m for Sn-9Zn-0.7Cu ternary alloys is higher than that of Sn-9Zn binary alloy, illustrating that the sensitivity parameter m for both compositions becomes temperature dependent.

The activation energy of steady creep at constant stresses was calculated using equation [17].

$$Q = R\left(\partial \ln \varepsilon_{st} / \partial\left(1/T\right)\right) \tag{3}$$

where R and T are the gas constant and absolute temperature, respectively. Moreover, the obtained results verify the equation of steady state creep [18-20]

$$\dot{\varepsilon}_{st} = c\left(\frac{\sigma}{d}\right)^{1/m} \exp\left(\frac{Q}{kT}\right) \tag{4}$$

where m = 0.5 for dislocation climb along grain boundaries [21] therefore, it is considered here that the higher elongation is attributed to the dislocation motion results in *GBS* and contained it during the deformation.

The activation energy of steady state creep was calculated from the relation between $\ln\dot{\varepsilon}_{st}$ and 1000/T at low and high temperature for Sn-9Zn eutectic and Sn-9Zn-0.7Cu alloys for five different applied stresses. The activation energies for the binary eutectic and ternary alloys have been found to be 21.99-24.73 and 16.06- 24.22 $kJ\,mol^{-1}$ in the low and high temperature regions, respectively see Fig.(13, 14). It is clear that activation enthalpies for Sn-9Zn binary alloys are more than ternary Sn-9Zn-0.7Cu alloys in low and high temperature regions see Table (2).

Table (2): Comparison of the steady state creep characteristics of the tested alloys.

Materials	(m)	ε'_{st}	Q ($kJmol^{-1}$)
Sn-9Zn	0.24 : 0.356	$5.52*10^{-7} : 1.39*10^{-5}$	21.99 : 24.73
Sn-9Zn-0.7Cu	0.26 : 0.372	$1.48*10^{-6} : 1.43*10^{-5}$	16.06 : 24.22

IV. Conclusion

The main conclusions to be drawn from this work are as follows:

1-The transient creep parameter *n and,* β increases with increasing the deformation temperature, their values of in case of Sn-9Zn-0.7Cu are more than that of Sn-9Zn

2-Steady-state strain rate $\dot{\varepsilon}_{st}$ increases with increasing the deformation temperature for the two tested alloys, the value of Steady-state strain rate $\dot{\varepsilon}_{st}$ for Sn-9Zn-0.7Cu is higher than that of Sn-9Zn

3- Strain rate sensitivity parameter m increases with increasing the deformation temperature for Sn-9Zn eutectic and Sn-9Zn-0.7Cu alloys. The value of m for Sn-9Zn-0.7Cu is higher than that of Sn-9Zn

4- The Sn-9Zn-0.7Cu ternary alloys show superior superplastic behavior in comparison with Sn-9Zn binary eutectic.

5- It is clear that activation enthalpies for Sn-9Zn binary alloys are higher than ternary Sn-9Zn-0.7Cu alloys in low and high temperature regions for transient and steady state creep regions.

6- A significant improvement in the creep resistance is achieved by 0.7Cu additions to the binary Sn–9Zn solder alloy.

References

[1] B.M. Guenin, R.C. Marrs, R.J. Molnar, IEEE transactions on components, Packaging Manufac. Technol. Part A 18 (1995) 749.

[2] J.H. Lau, Ball Grid Array Technology, SMTnet, 1995.

[3] M. Cosle, E. Kastberg, G. Matin, in: Surface Mount International, Proceedings, 1996, pp. 89–94.

[4] O. Unal, J.C. Foley, Mater. Sci. Lett. 20 (2001) 1585.

[5] W.K. Liou, Y.W. Yen, K.D. Chen, J. Alloys Compd. 479 (2009) 225–229.

[6] X. Wei, H. Huang, L. Zhou, M. Zhang, X. Liu, Mater. Lett. 61 (2007) 655–658.

[7] S.H.Wang, T.S. Chin, C.F. Yang, S.W.Chen, C.T.Chuang, J. Alloys Compd. 497 (2010) 428–431.

[8]A.A. El-Daly, Y. Swilem, M.H. Makled, M.G. El-Shaarawy, A.M. Abdraboh, J. Alloys, Compd. 484 (2009) 134–142.

[9] A.A. El-Daly, A.E. Hammad, Mater. Sci. Eng. A (2010), doi:10.1016/j.msea 078.

[10] R.M. Shalaby, Cryst. Res. Technol. (2010), doi:10.1002/crat.201000022.

[11] A.A. El-Daly, A.M. Abdel-Daiem, M. Yousf, Mater. Chem. Phys. 71 (2001) 111.

[12] A.A. El-Daly, A.M. Abdel-Daiem, M. Yousf, Mater. Chem. Phys. 74 (2002) 43.

[13] M.S. Saker, A.Z. Mohamed, A.A. El-Daly, A.M. Abdel-Daiem, A.H.Bassyouni, Egypt. J. Solids B2 (1990) 34.
[14]Hucheng Pan, He Fu, Yuping Ren, Qiuyan Huang, Zhengyuan Gao, Jia She, Effect of Cu/Zn on microstructure and mechanical properties of extruded Mg–Sn alloys, Mater. Sci. Technol, 2016, 32,1240.
[15] J. Friedel, Dislocations, Pergamon Press, London, 1964, p. 304
[16] O. Takahashi, Y. Terada, M. Takeyama, T. Matsuo, Mater. Sci. Eng. A 329 (2002) 835.
[17] J.Weertman, Rate Processes in Plastic Deformation of Materials, (ASM, 1975, 315).
[18] A. Fawzy, N. Habib, M. Sobhy, E.Nassr,G. Saad, Materials Science and Technology 24, 2008, 488-494.
[19]A.A. El-Daly, A.E. Hammad, Journal of Alloys and Compounds 509, 2011, 8554-8560.
[20] A. Fawzy, S.A.Fayek, M.Sobhy, E.Nassr, M.M. Mousa, G. Saad, J Mater Sci, Mater Electron, 24, 2013, 3217.
[21]A.A. El-Dalya, A.Z. Mohamad, A. Fawzy, A.M.El-Taher, Materials Science and Engineering A 528, 2011, 1055 -1062.

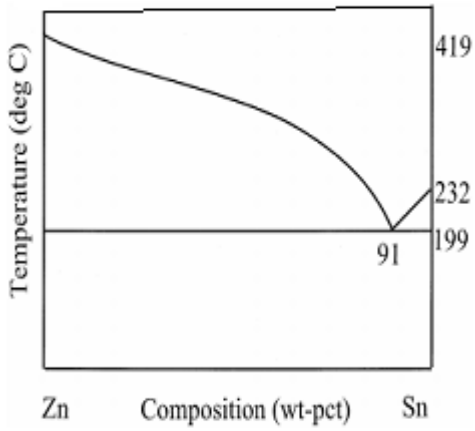

Fig.1. Phase diagram for Sn–9Zn binary system.

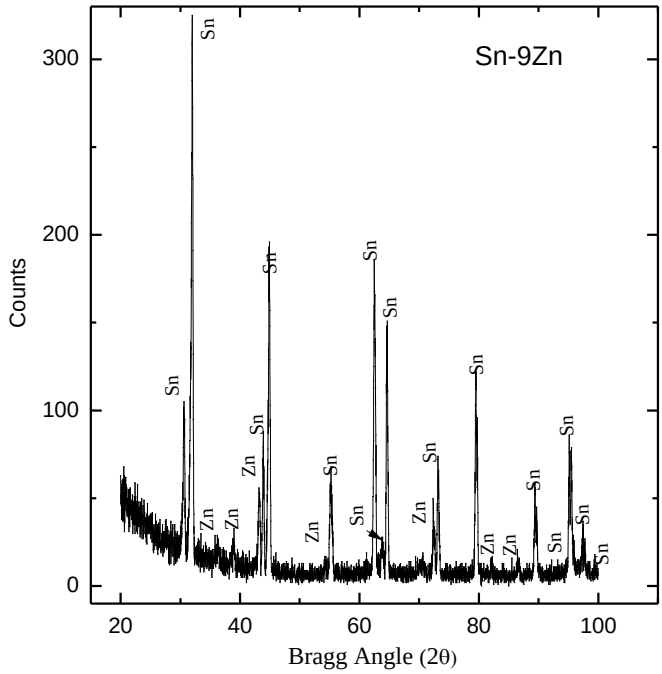
Sn-9Zn
Counts
Bragg Angle (2θ)
0
100
200
300
20
40
60
80
100
Sn
Zn

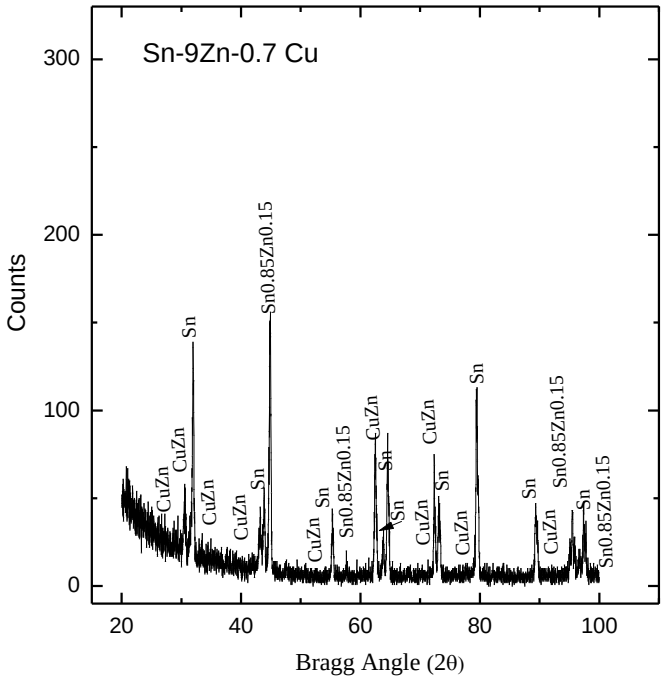

Fig. 2.(a) XRD pattern for Sn-9Zn binary alloy are mainly composed of β-Sn phase and precipitated Sn_5Zn_8 phase and, (b) Sn-9Zn-0.7Cu ternary alloys containing Cu exhibited additional IMCs such as Cu_6Sn_5.

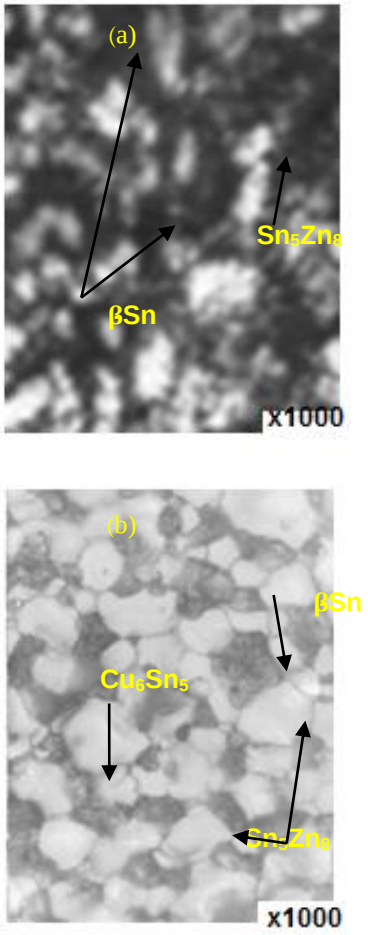

Fig.(3)The OM images of the two alloys (a) a typical eutectic Sn–9Zn microstructure composed of light gray areas of Sn_5Zn_8 IMCs and dark network-like eutectic regions of β-Sn grain boundaries. In (b), the appropriate content of Cu in the Sn–9Zn solder was found to improve the microstructure of the alloy. The primary Cu_6Sn_5 IMCs might act as heterogeneous nucleation sites for β-Sn dendrites upon solidification and are able to refine the grain size of Sn–9Zn alloy, the microstructure in the ternary alloys must be uniform and finer grain size.

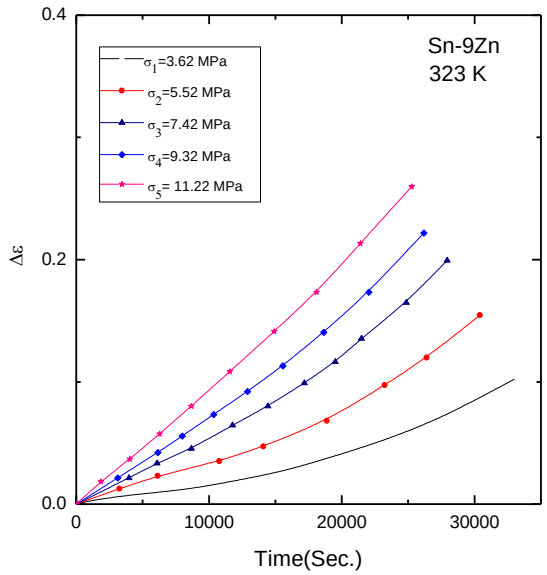
Sn-9Zn
323 K
σ1=3.62 MPa
σ2=5.52 MPa
σ3=7.42 MPa
σ4=9.32 MPa
σ5= 11.22 MPa
Δε
0.0
0.2
0.4
0
10000
20000
30000
Time(Sec.)

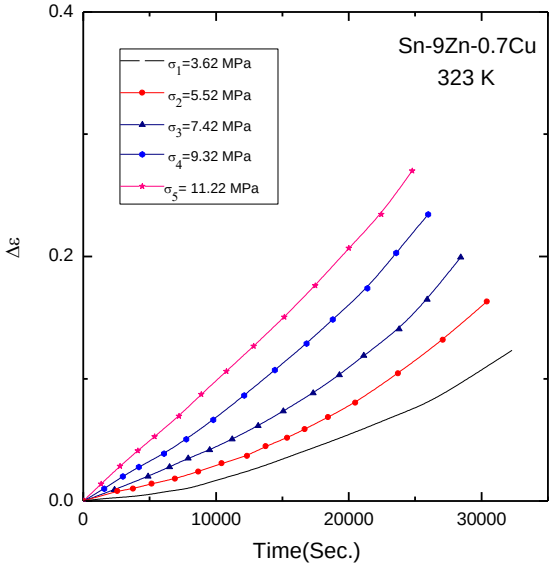

Fig.(4a): Isothermal Creep Curves at 323 K, at different applied stresses for Sn–9Zn eutectic and Sn–9Zn-0.7Cu alloys.

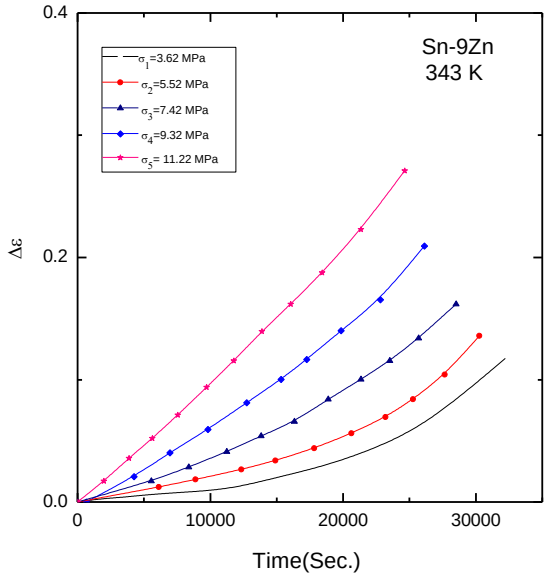

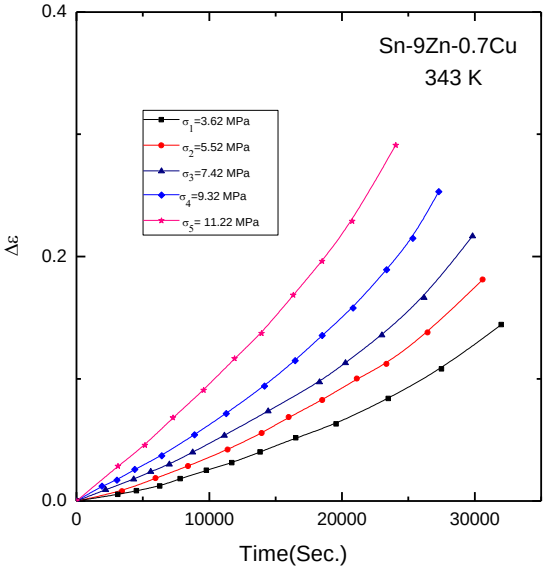

Fig.(4b): Isothermal Creep Curves at 343 K, at different applied stresses for Sn–9Zn eutectic and Sn–9Zn-0 . 7 C u alloys.

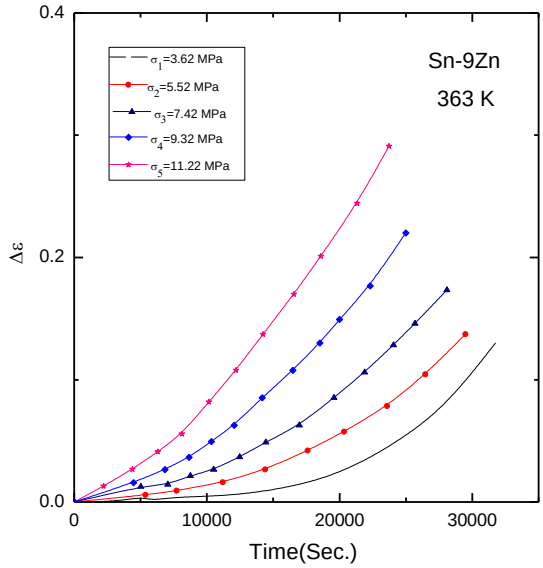

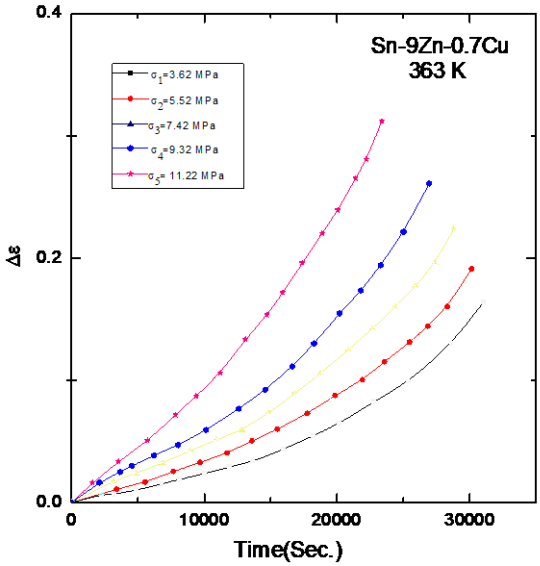

Fig.(4c): Isothermal Creep Curves at 363 K, at different applied stresses for Sn–9Zn eutectic and Sn–9Zn-0 . 7 C u alloys

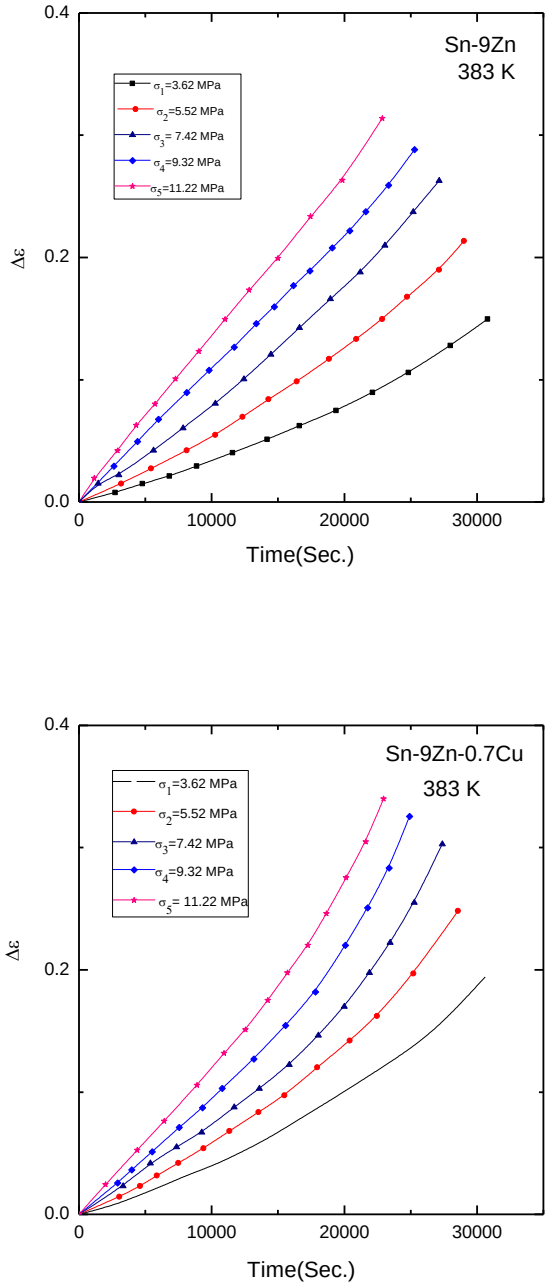

Fig.(4d): Isothermal Creep Curves at 383 K, at different applied stresses for Sn–9Zn eutectic and Sn–9Zn-0 . 7 C u alloys

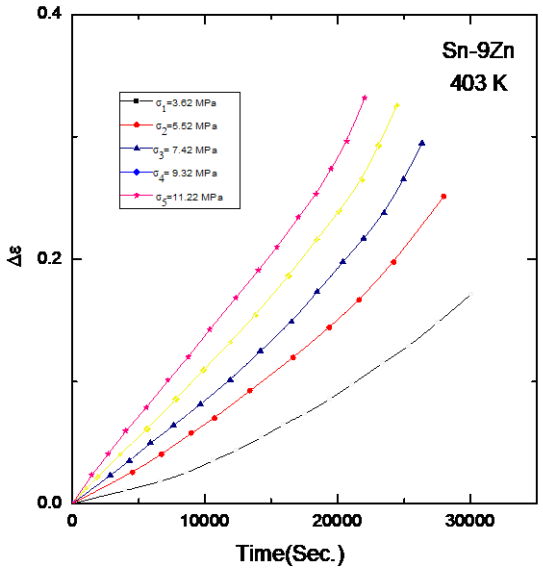

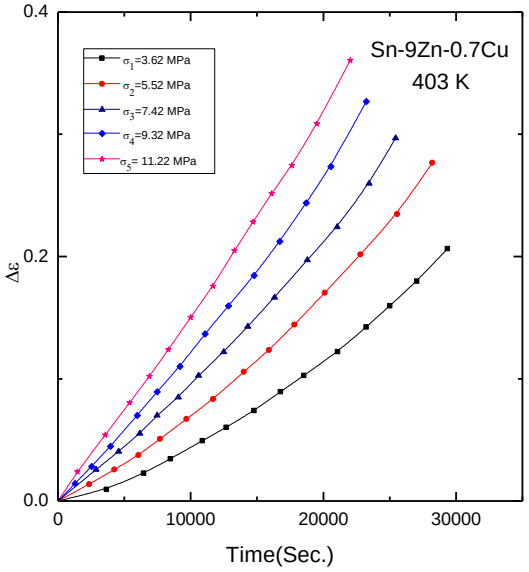

Fig.(4e): Isothermal Creep Curves at 403 K, at different applied stresses for Sn–9Zn eutectic and Sn–9Zn-0 . 7 C u alloys

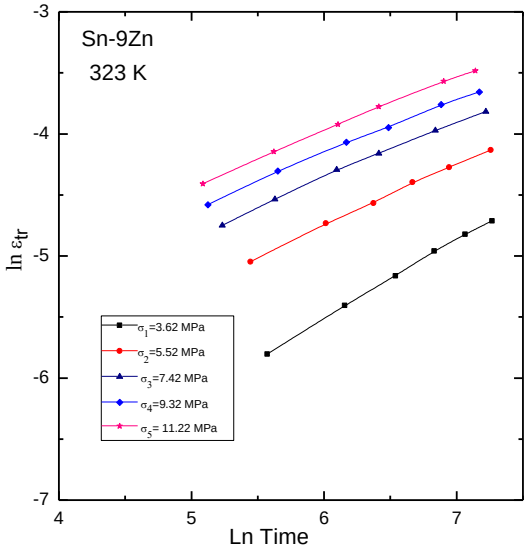

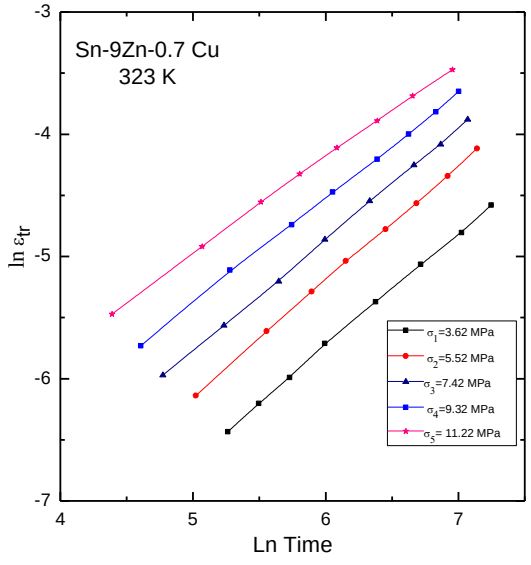

Fig.(5a): Relation between ln(ε_{tr}) and lnt for Sn–9Zn eutectic and Sn–9Zn-0 . 7 C u alloys, at 323K and different stresses.

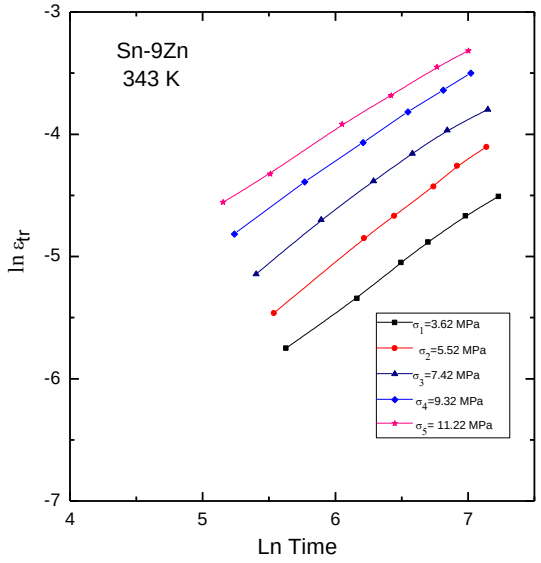

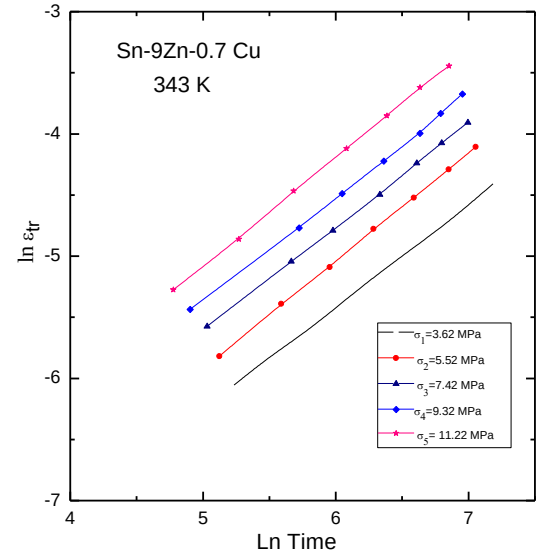

Fig.(5b): Relation between ln(ε_{tr}) and lnt for Sn–9Zn eutectic and Sn–9Zn-0.7Cu alloys, at 343K and different stresses.

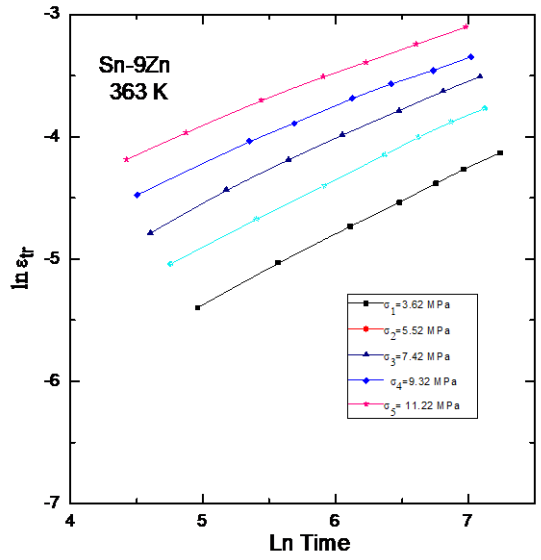

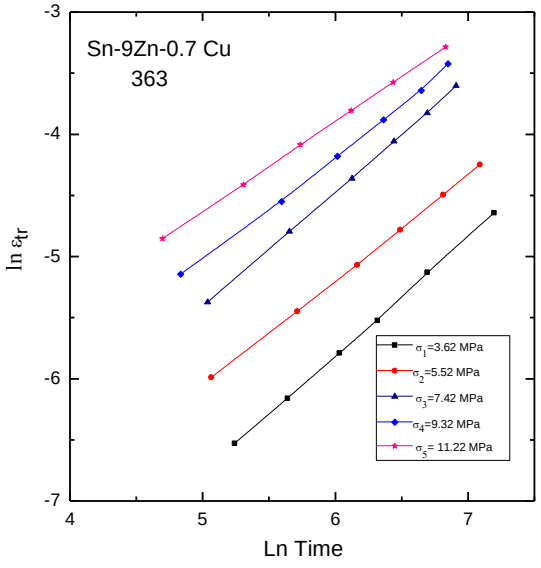

Fig.(5c): Relation between ln(εtr) and lnt for Sn–9Zn eutectic and Sn–9Zn-0.7Cu alloys, at 363K and different stresses.

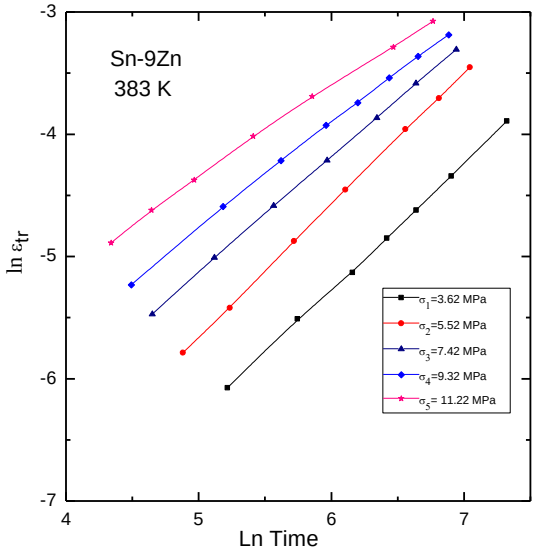

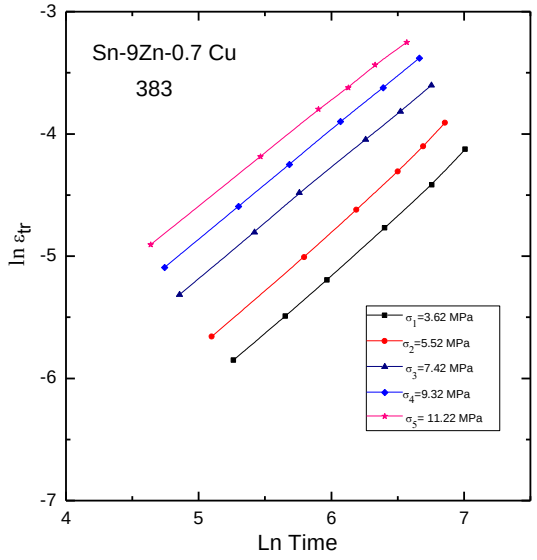

Fig.(5d): Relation between ln(ε_{tr}) and lnt for Sn–9Zn eutectic and Sn–9Zn-0.7Cu alloys, at 383K and different stresses.

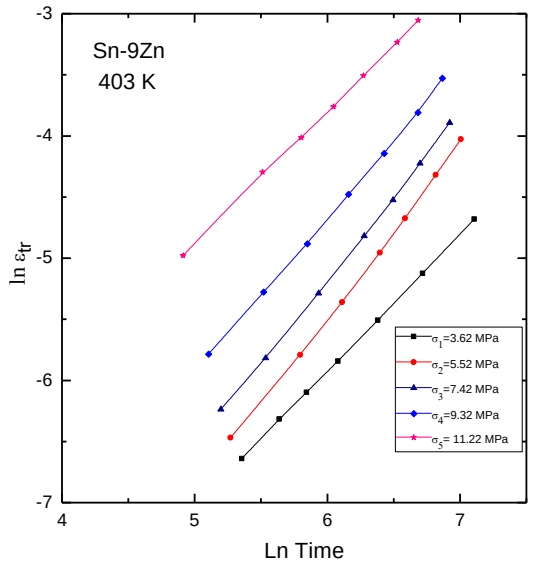

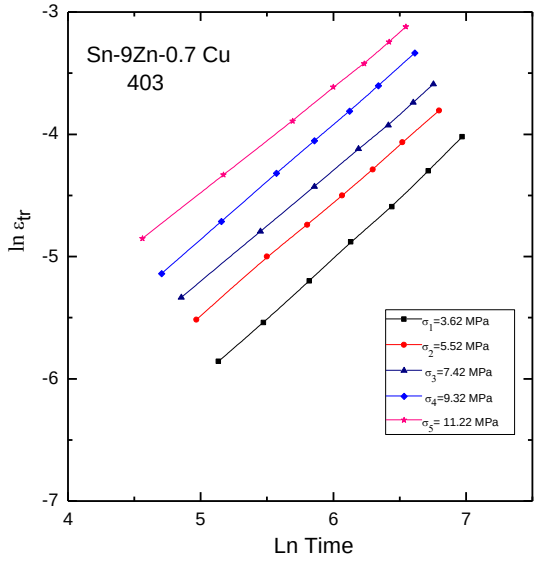

Fig.(5e): Relation between ln(ε_{tr}) and lnt for Sn–9Zn eutectic and Sn–9Zn-0.7Cu alloys, at 403K and different stresses.

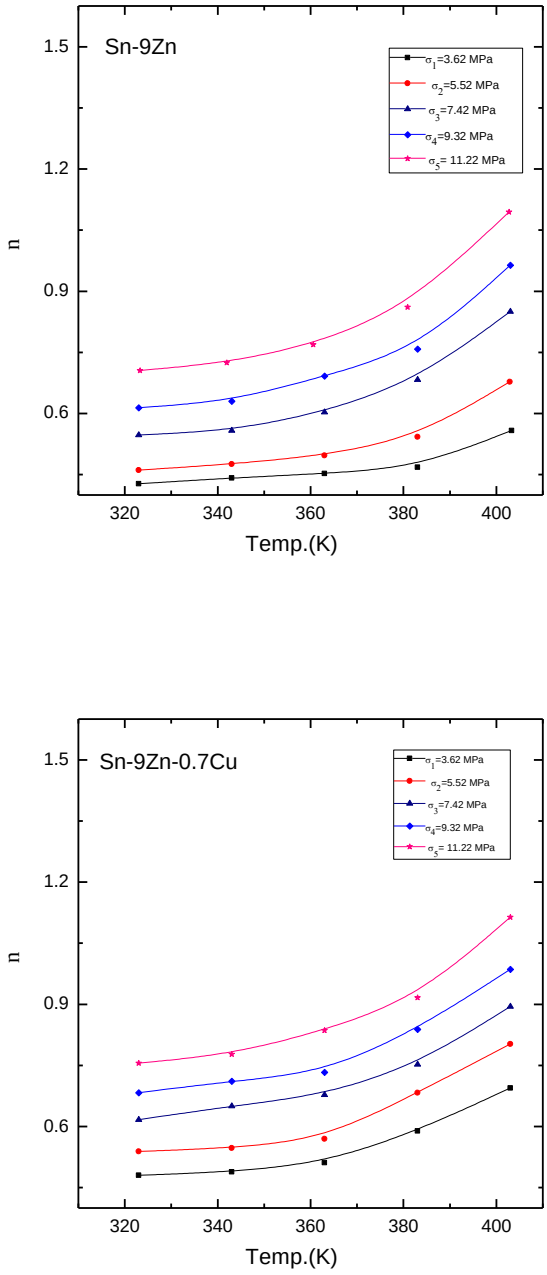

Fig.(6):The dependence of the parameters, n, on the working temperature at different applied stresses for Sn–9Zn eutectic and Sn–9Zn-0.7Cu alloys.

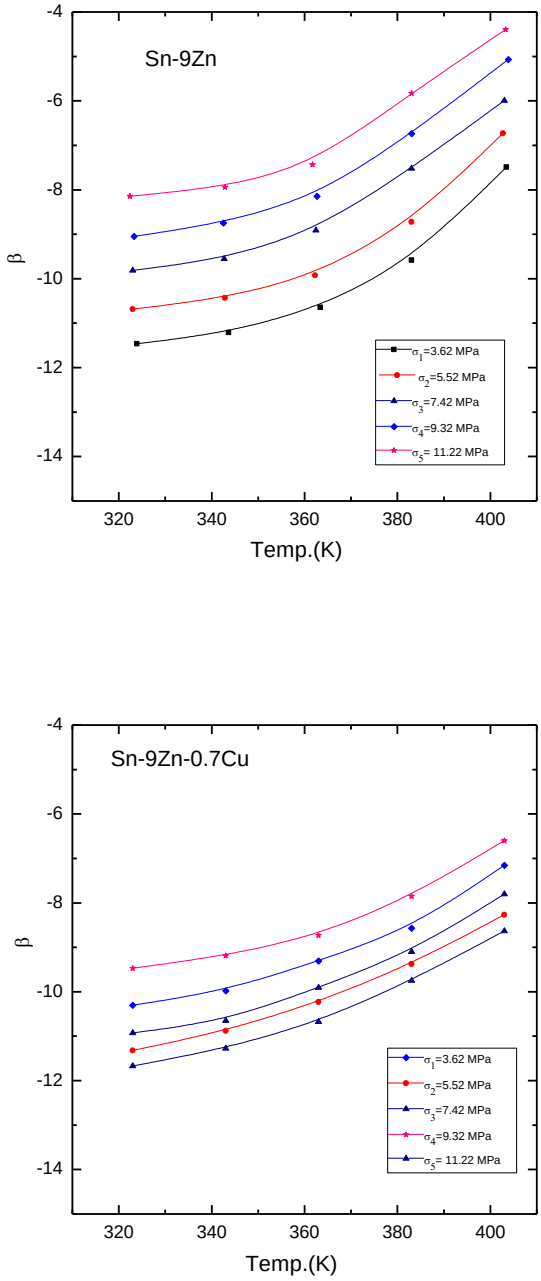

Fig.(7):The dependence of the parameters, β, on the working temperature at different applied stresses for Sn–9Zn eutectic and Sn–9Zn-0.7Cu alloys.

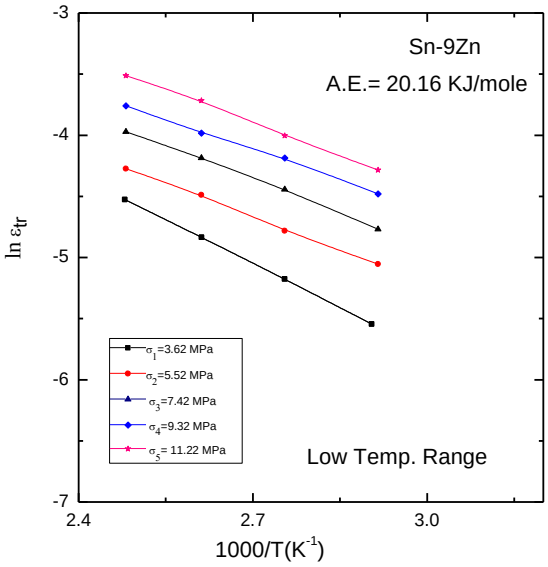

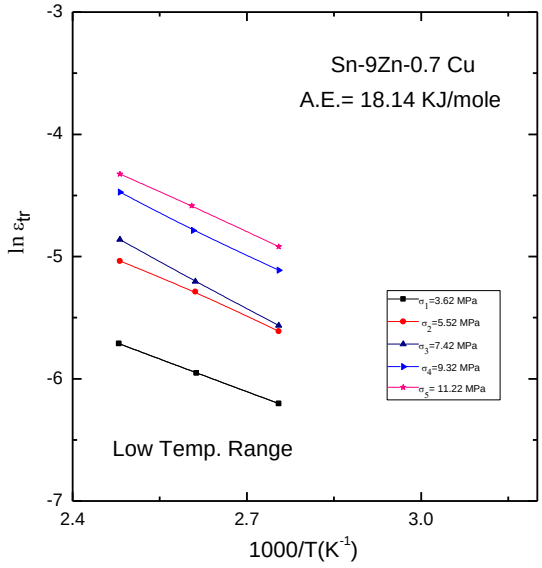

Fig.(8): The relation between $Ln\varepsilon_{tr}$ and 1000/T at different applied stresses for Sn-9Zn eutectic and Sn-9Zn-0.7Cu alloys at low Temp.

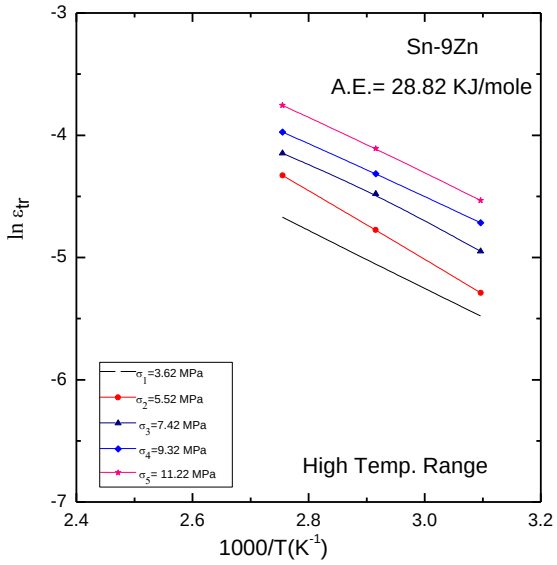

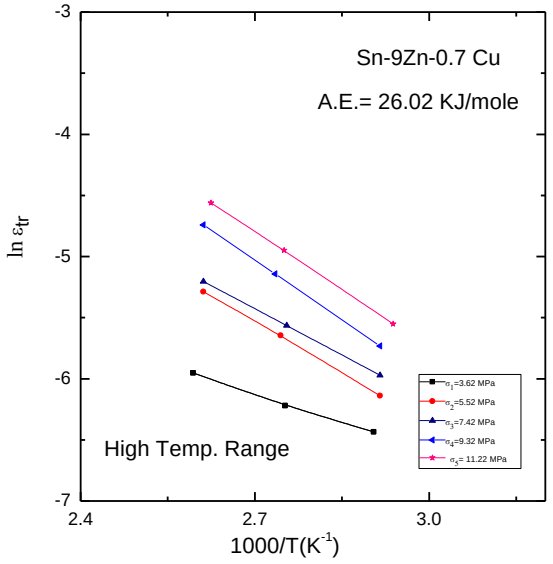

Fig.(9): The relation between $Ln\varepsilon_{tr}$ and 1000/T at different applied stresses for Sn-9Zn eutectic and Sn-9Zn-0.7Cu alloys at high Temp.

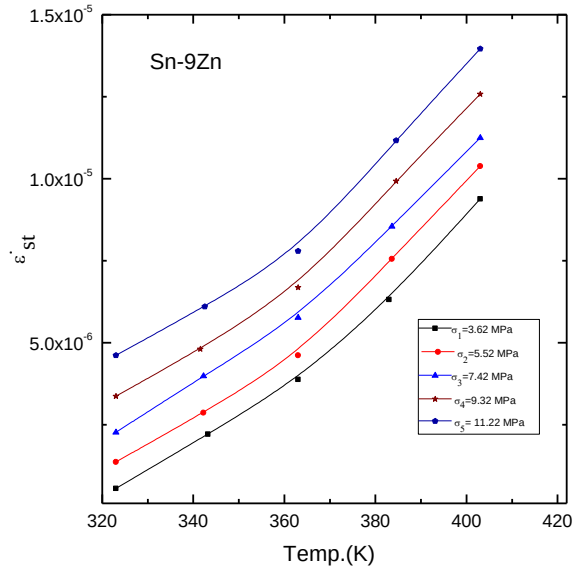

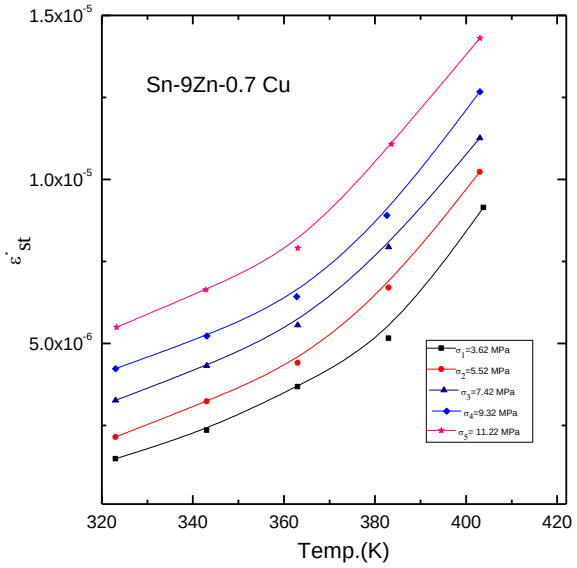

Fig.(10): Steady-state strain rate $\dot{\varepsilon}_{st}$ as a function of creep temperature for Sn-9Zn eutectic and Sn-9Zn-0.7Cu alloys.

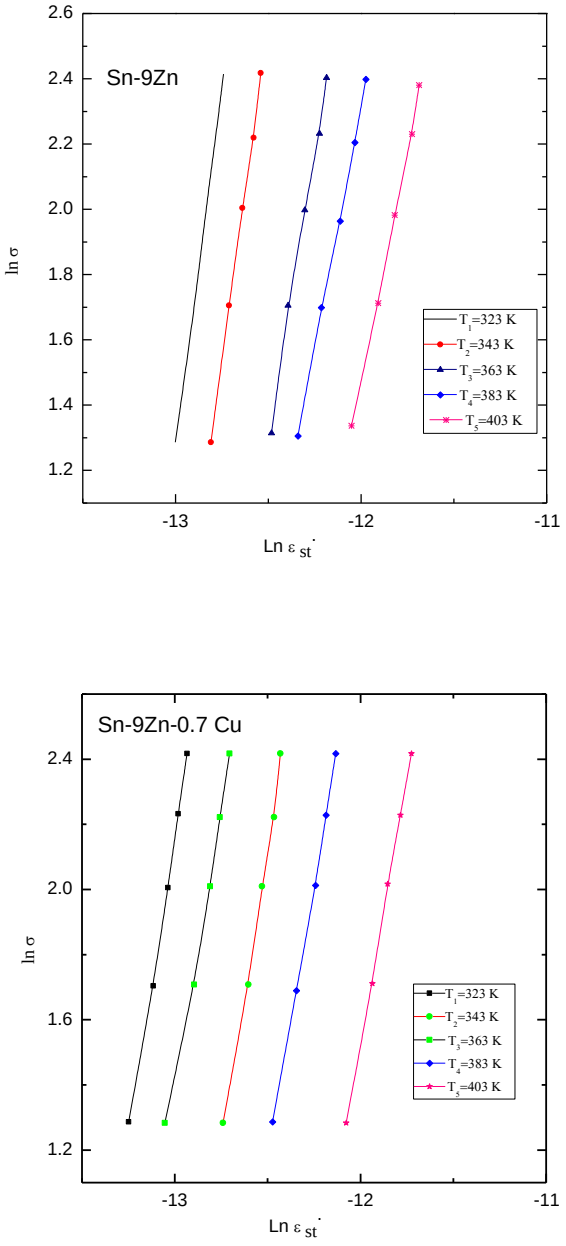

Fig.(11): Strain rate–stress relationship for Sn-9Zn eutectic and Sn-9Zn-0.7Cu alloys.

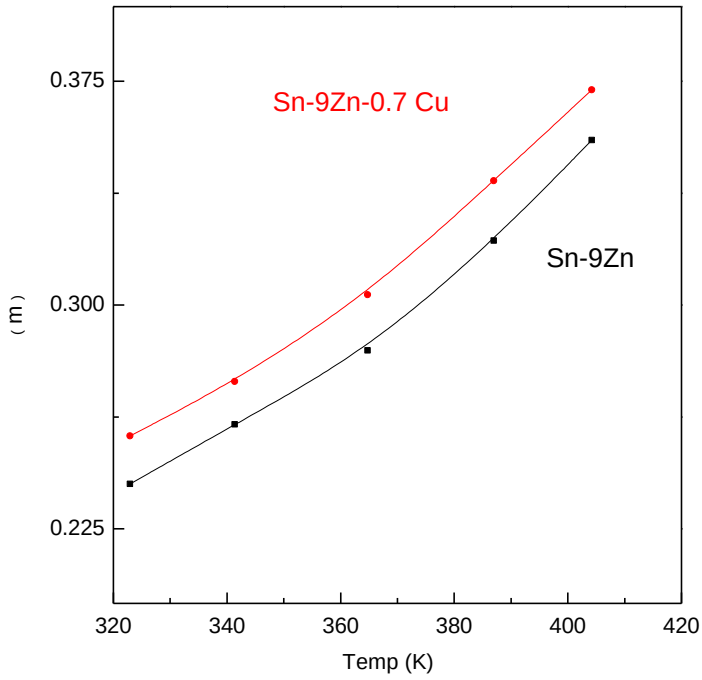

Fig.(12): Strain rate sensitivity parameter m as a function of creep temperature Sn-9Zn eutectic and Sn-9Zn-0.7Cu alloys.

.

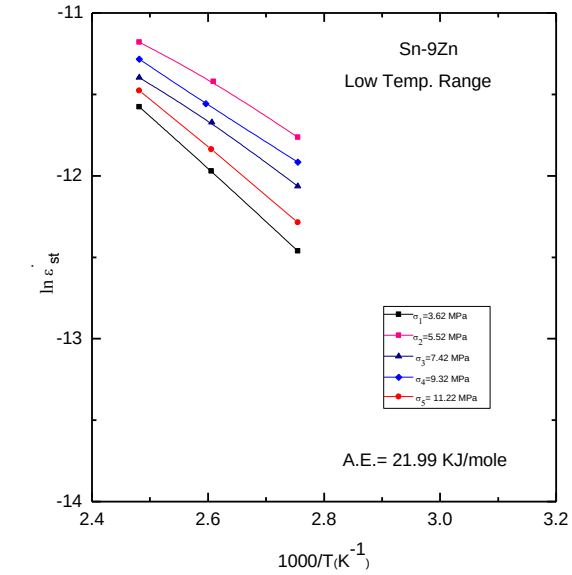

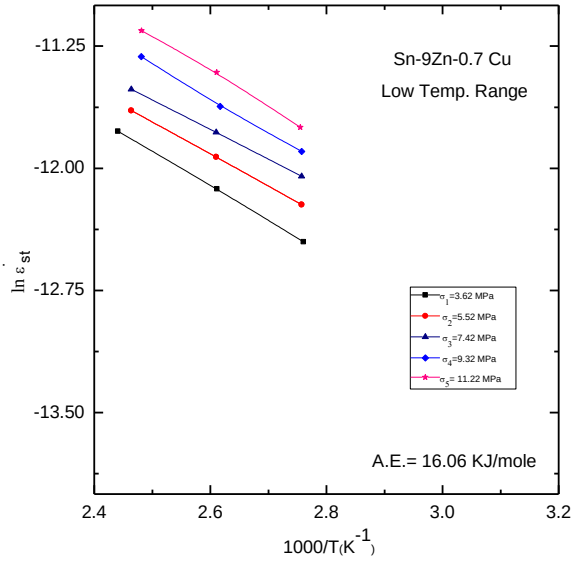

Fig.(13): The relation between Ln$\dot{\varepsilon}_{st}$ and 1000/T at different applied stresses for Sn-9Zn eutectic and Sn-9Zn-0.7Cu alloys at low Temp.

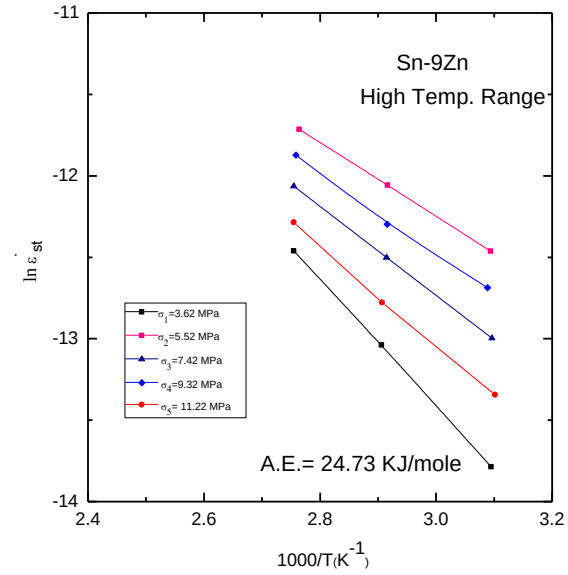

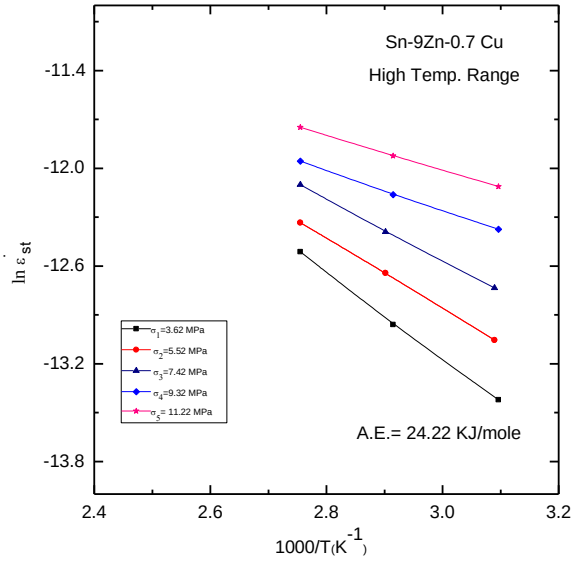

Fig.(14): The relation between $Ln\varepsilon_{st}$ and 1000/T at different applied stresses for Sn-9Zn eutectic and Sn-9Zn-0.7Cu alloys at high Temp.